

ENC-2020-0656

**INTEGRATING CONCENTRATED SOLAR POWER WITH
DESALINATION: MODELING AND THERMODYNAMIC ANALYSIS**

Vítor Silva Medeiros

Solidônio Rodrigues de Carvalho

Universidade Federal de Uberlândia, Faculdade de Engenharia Mecânica, 38400-902, Santa Mônica, Uberlândia, MG – Brasil
vitormedeiros@ufu.br
solidonio@ufu.br

Valério Luiz Borges

Universidade Federal de Uberlândia, Faculdade de Engenharia Mecânica, 38400-902, Santa Mônica, Uberlândia, MG – Brasil
valerioluizborges@ufu.br

Abstract. *The availability of freshwater worldwide is likely to decrease while the demand increase, due in part to climate change. Countries that can afford it have increasingly turned to desalination, an extremely energy intensive process that extracts salt from seawater. Fortunately, most arid regions generally reside in regions of very solar insolation (most in the Mediterranean Sea or Middle East). Integrating Concentrating Solar Power (CSP) and desalination technologies is one way to produce simultaneously potable water and energy, besides offset many of negative impacts of running desalination plants. The model developed in the context of this work is suitable for use in optimization of water and power cogeneration systems. In particular a Multi-Effect Distillation (MED) system was modeled in a modular method and solved with an equation-oriented solver. Moreover, a simplified Rankine cycle was designed and integrated with the desalination plant. Data from other MED models using a thermal vapor compressor (TVC) was used for comparison and development of the models. The results show that these tools are a useful addition to a cogeneration system optimization process.*

Keywords: *Model, desalination, CSP, MED, cogeneration*

1. INTRODUCTION

Desalination of seawater and brackish water is receiving special concern due to scarcity of water in many places in the world. As a result of population growth around the world and constant amount of freshwater in the planet, the need to develop new sources of freshwater arises. Moreover, accordingly to U.S. Energy Information Administration (2019) the energy consumption will rise 50 % between 2018 and 2050, as a consequence of rapid population growth and strong economic development. The need for energy and water are intricately connected since energy is mandatory for the treatment, production, collection, and delivery of water, in the same way all forms of energy require some amount of water as part of their production, generation or processing. Concentrating Solar Power (CSP) and desalination processes can be a solution to deal with problems of water scarcity and sustainable electricity production in many zones around the globe, where both these commodities are in short supply (F. Trieb, 2007). Proven technologies like Multi-effect distillation (MED), Multi-Stage Flash (MSF), Reverse Osmosis (RO) are the most reliable and efficient methods to provide freshwater by the desalination process. J. Blanco et al. (2013) stated that combining CSP and desalination plants is a very attractive solution for a few reasons, like the technological synergies identified to potentially reduce the cost of combined power and water. Additionally, the exportation of electricity to other countries can be justified and, mutually the basic need of the local population can be fulfilled by locally distributing the water. However, some technical aspects remain unsolved, development and demonstration works are necessary to define the best concepts and systems.

Studies towards basic integrated power and desalination plants design have been published, S. Casimiro et al. (2014) as an example developed a tool to simulate the cogeneration of water and electricity with Concentrating Solar Power (CSP) and Forward Feed Multi-Effect Distillation (FF-MED) plants and showed that the electrical performance of the CSP+MED is only 5 % lower than the conventional CSP+Wet Cooling plant, but with the advantage of producing freshwater. In other analysis J. Blanco et al. (2013) showed that at 18 kPa in the turbine outlet conditions, the configuration involving MED and CSP technologies for arid regions is more efficient thermodynamically than the coupling of CSP plant with reverse osmosis (RO) and needs a smaller solar field for the same production of electricity. R. Olwig et al. (2012) in a techno-economic analysis of CSP+MED and CSP+RO plant configurations for a site in Isreal (Ashdod) and Jordan (Aqaba), showed that those configurations can be a realistic economic future option for the freshwater production

to meet the demand of the Middle East and North Africa region, although it has to be noted that water costs of the project can only be evaluated based on detailed information accounting all boundary conditions.

The focus of this study is to obtain a tool that can simulate the physical performance of a cogeneration plant combining CSP and MED technologies, for a pre-design stage analysis. The models were solved using a simultaneous equation solver that simplifies the coding complexity and reduces approximations and assumptions.

2. DESCRIPTION OF THE COGENERATION SYSTEM

This analysis considered a parabolic trough (CSP) plant combined with a multi-effect distillation (MED) configuration as shown in Fig. 1. The performance simulation focused on the desalination plant and the steam part of power generation cycle. For this work a reheat Rankine power block model for parabolic trough CSP plants was chosen, generating 100 MW_e. In this simulation a standalone MED plant and a MED plant using a thermal vapor compressor TVC were designed.

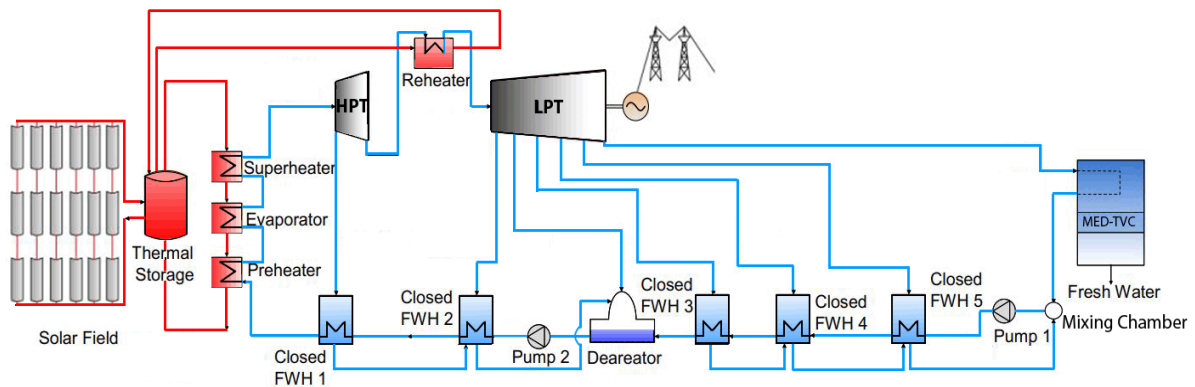


Figure 1. Diagram of the cogeneration system CSP+MED analyzed in this study.

2.1 MED desalination system

The MED model is based on Mistry et al. (2013) work that provides a more accurate description of the MED process through relying on fewer assumptions and simplifications. In this model the energy and mass balance equations are inputted much as one would write them on paper, then the simultaneous equation solver recognizes and groups the equations in an iterative method that find the solution. Seawater is approximated as an incompressible fluid, properties are evaluated as a function of temperature and salinity, as presented in the Sharqawy et al. (2010) study. All liquid water are modeled using a seawater property functions, while vapor and distillate water are modeled with 0 salinity. A simple view of the MED with thermal vapor compression TVC is illustrated in Fig. 2.

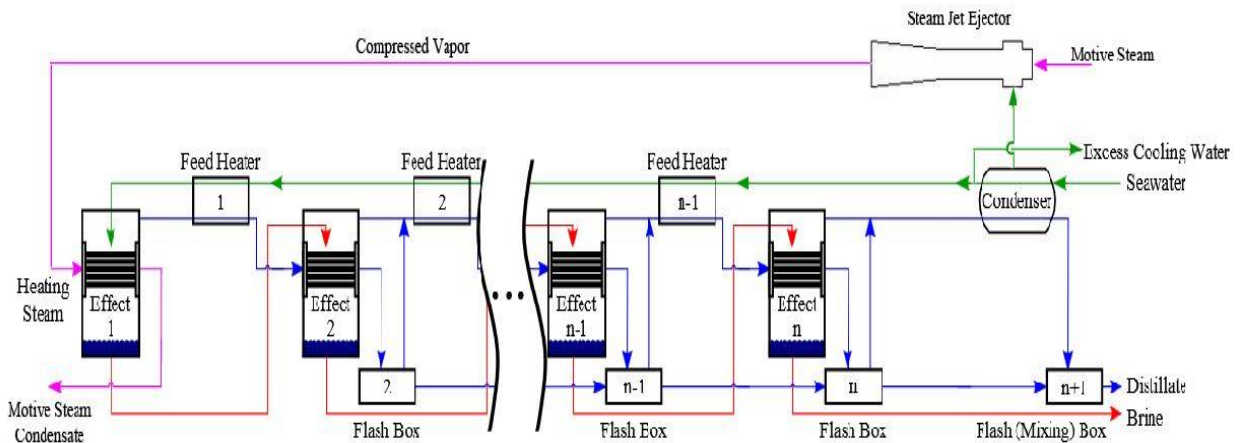


Figure 2. View of the components connections between each effect in an MED-TVC system.

Mass and energy are specified for the different components in the system. The main equations are stated here to illustrate the changes upon adding the TVC to the existing model, more information about the MED model is deeply detailed in Mistry et. (2013) work. The following system assumptions are considered in this analysis:

- Steady-state operation.
- Distillate is pure water (salinity of product water is 0 g/kg).
- Exchanger area in the effects is just large enough to condense vapor to saturated liquid.
- Seawater is an incompressible liquid and the properties are only a function of temperature and salinity.
- Energy losses to the environment are negligible.
- Non-equilibrium allowance (NEA) is negligible.
- Brine (liquid) and distillate (vapor) streams leave each effect at that effect's temperature.
- Distillate vapor is slightly superheated.
- The overall heat transfer coefficient is averaged over the length of an exchanger.
- The overall heat transfer coefficient in each effect, feed heater, and condenser is a function of temperature only.

Also, for the design analysis, a few system characteristics must be specified:

- Temperature of the last effect, or a terminal temperature difference between the last effect and the condenser.
- Mass flow rate of the distillate, feed, or brine.
- Maximum allowable salinity (or recovery ratio).
- Temperature rise in the condenser.
- Minimum TTD in the feed heaters.

The overall system mass and salt balance is determined by Eq. (1) and Eq. (2).

$$\dot{m}_F = \dot{m}_B + \dot{m}_D \quad (1)$$

$$\dot{m}_F \cdot X_F = \dot{m}_B \cdot X_B \quad (2)$$

where, \dot{m} : mass flow rate, F : feed, D : distillate, B : brine, X_B : brine stream leaving the system and X_F : salinity of feedwater.

The heat transfer surface area in each effect is expressed by Eq. (3). An energy balance and logarithmic mean temperature difference are used to calculate the required heat transfer in the condenser A_c expressed by Eq. (4).

$$\dot{m}_{Dc} \cdot \Delta h_{Dc} = A_e \cdot U_e (T_c - T_e) \quad (3)$$

where \dot{m}_{Dc} : distillate that will condense in effect, Δh_{Dc} : change in enthalpy of the distillate, A_e : heat transfer area in effect, U_e : overall heat transfer coefficient in effect, T_c : condensing temperature, T_e : temperature of the effect.

$$\dot{m}_{cond} \cdot (h_{sw}^{out} - h_{sw}^{in}) = A_c \cdot U_c \frac{T_{sw}^{out} - T_{sw}^{in}}{\ln \frac{T_c - T_{sw}^{in}}{T_c - T_{sw}^{out}}} \quad (4)$$

where \dot{m}_{cond} : flow rate of seawater in condenser, h_{sw}^{out} , T_{sw}^{out} and h_{sw}^{in} , T_{sw}^{in} the enthalpy and temperature of seawater that enters and leaves the condenser, U_c : overall heat transfer coefficient in the condenser. The overall heat transfer coefficient in Eq. (3), (4) are calculated using correlations from El-Dessouky and Ettouney (2002) showed in Eq. (5), (6).

$$U_e = 10^{-3} \cdot [1939.1 + 1.40562 \cdot (T_c) - 0.0207525 \cdot (T_c)^2 + 0.0023186 \cdot (T_c)^3] \quad (5)$$

$$U_c = 10^{-3} \cdot [1617.5 + 0.1537 \cdot (T_c) + 0.1825 \cdot (T_c)^2 - 0.00008026 \cdot (T_c)^3] \quad (6)$$

The main evaluation parameters of MED model are performance ratio (PR), defined as the proportion between the distillate and motive steam flow rates, specific area (sA) calculated by the summation of the heat transfer and condenser areas, and specific cooling water flow rate defined as the ratio between coolant flow and distillate produced rates expressed by Eq. (7), (8), (9) respectively.

$$PR = \frac{\dot{m}_D}{\dot{m}_M} \quad (7)$$

$$sA = \frac{(\Sigma A_e + \Sigma A_{fh} + \Sigma A_c)}{\dot{m}_D} \quad (8)$$

$$sm_{cw} = \frac{\dot{m}_{cw}}{\dot{m}_D} \quad (9)$$

where, A_{fh} : area of feed heater. More details about feed heat and condenser energy and mass balance, as well as match stream between components are presented in Mistry et al. (2013) study.

The steam jet ejector is modeled by the model developed by El-Dessouky and Ettouney (2002) and Power (1994). The entrainment ratio, Ra , defined as the ratio between the motive steam flow rate and the entrained flow rate is calculated from Eq. (10).

$$Ra = 0.296 \cdot \frac{(P_s)^{1.19}}{(P_{ev})^{1.04}} \cdot \left(\frac{P_m}{P_{ev}}\right)^{0.015} \cdot \left(\frac{PCF}{TCF}\right) \quad (10)$$

where, P_m , P_{ev} and P_s are the pressure of motive steam, entrained vapor and compressed vapor respectively, TCF is the entrained vapor temperature correction factor and PCF is the motive steam pressure correction factor, calculated by Eq. (11) and Eq. (12).

$$PCF = 3 \cdot 10^{-7} \cdot (P_m)^2 - 0.0009 \cdot (P_m) + 1.6101 \quad (11)$$

$$TCF = 2 \cdot 10^{-8} \cdot (T_{ev})^2 - 0.0006 \cdot (T_{ev}) + 1.0047 \quad (12)$$

where P_m is in kPa and T_{ev} is in °C. The previous correlations are valid only for ejectors operating with steam working in the limits of $Ra \leq 4$, $100 \text{ kPa} \leq P_m \leq 3500 \text{ kPa}$ and $1.8 \leq Cr \leq 6$ (El-Dessouky and Ettouney, 2002). The compression ratio Cr is given by Eq. (13)

$$Cr = \frac{P_s}{P_{ev}} \quad (13)$$

2.2 Reheat Rankine cycle

As is shown in Fig. 1 a reheat Rankine cycle is considered, similar to the configuration proposed by J. Blanco et al. (2013). The cycle is modeled using energy and mass governing equations solving the system of equations simultaneously. The Rankine cycle model is solved relying on the following assumptions:

- Steady-state operation.
- No losses to the environment.
- Ideal feedwater heaters are considered.
- Pressure drops are excluded.

The steam turbine temperature and pressure conditions, Tab. 1, are based on similar values of a commercial turbine designed for CSP, power plants and seawater desalination plants applications.

Table 1. Steam inlet conditions and parameters of the turbine modeled.

Parameter	Value
Pressure (Mpa)	16
Temperature (°C)	565
HPT isentropic efficiency	85 %
LPT isentropic efficiency	85 %
Generator efficiency	99 %

Feedwater heating is applied to enhance the cycle efficiency. Steam is bled from the turbine and by transferring the heat to the feedwater, less external heat is required to generate steam. Four closed and one contact feed heater are implemented into the Rankine cycle design.

3. RESULTS AND DISCUSSION

3.1 Parametric comparison of MED models

Firstly, the present MED model based on Mistry et. (2013) work is compared to several researchers like Darwish (2008), El-Sayed (1980) and other models illustrated in Fig. 3. The results show that the added benefit of number of effects on the performance ratio decrease for a high number of effects as seen by the PR behavior of Mistry, El-Sayed, El-Dessouky Detailed, and present model. The minor divergence between the present and Mistry model is justified by a few adjustments in the model like the use of Eq. (4) and Eq. (6) as proposed by El-Dessouky and Ettouney (2002).

The MED-TVC model is validated through comparing the results with (El-Dessouky and Ettouney, 2002) and (Khalid et al., 2018). A good agreement is shown in Tab. 2, the maximum deviation 13.20 % was observed in the specific cooling water flow rate. Moreover, a parametric study is conducted in which the model of the present work is compared to MED-

TVC (El-Dessouky and Ettouney, 2002) model. Figure 4 and 5 illustrate the performance ratio and specific flow rate of cooling water evaluated for each of the models while varying the number of effects and steam temperature. As is shown the increase in the number of effects is one of the strongest determinants of rise in performance. On the other side, the decrease in the performance ratio of the MED-TVC system at higher temperatures is due to the larger amount of motive steam used to achieve the determined compression range. In addition, high temperatures followed by an increase of amount of motive steam also increases the system thermal load and the required amount of cooling water per kg of distillate product.

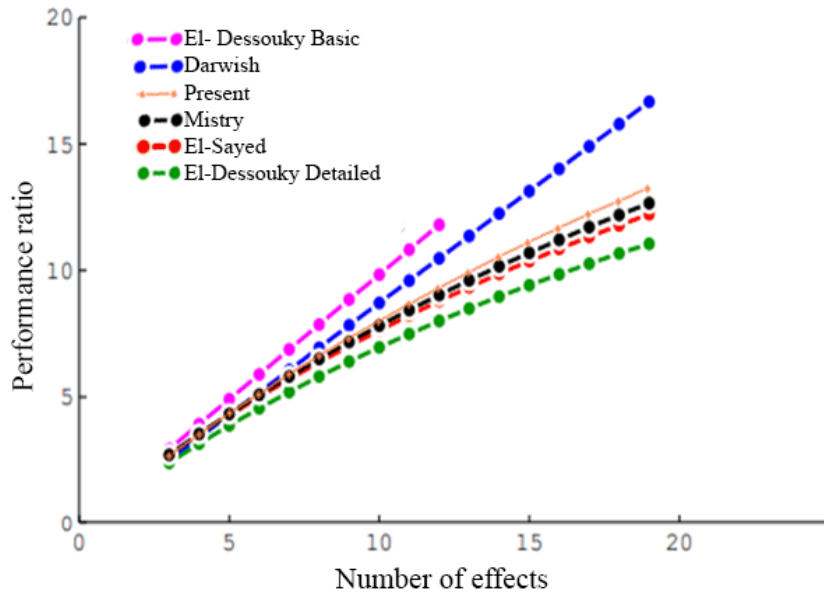


Figure 3. Behavior of performance ratio with increase of number of effects.

Table 2. Model validation by comparing results with (El-Dessouky and Ettouney, 2002) and (Khalid et al., 2018) studies

Parameter	Present model MED/FF/TVC	Khalid MED/FF/TVC Model	Percentage difference	El-Dessouky MED/FF/TVC Model	Percentage difference
Number of Effects	4	4	-	4	-
Intake Seawater Salinity (ppm)	42000	42000	-	42000	-
Rejected Brine Salinity (ppm)	70000	70000	-	70000	-
Intake Seawater Temperature (°C)	25	25	-	25	-
Feed Seawater Temperature (°C)	35	35	-	35	-
Heating Steam Temperature (°C)	60	60		60	
Rejected Brine Temperature (°C)	40	40		40	
Ra	2.313	2.199	4.93 %	2.228	3.67 %
Cr	3.15	3.006	4.57 %	3.144	0.19 %
sm _{cw}	7.82	6.788	13.20 %	6.819	12.80 %
PR	5.184	5.275	1.76 %	5.26	1.47 %
Ac	31.85	32.92	3.36 %	32.79	2.95 %
sA	350.1	346.3	1.09 %	345.76	1.24 %

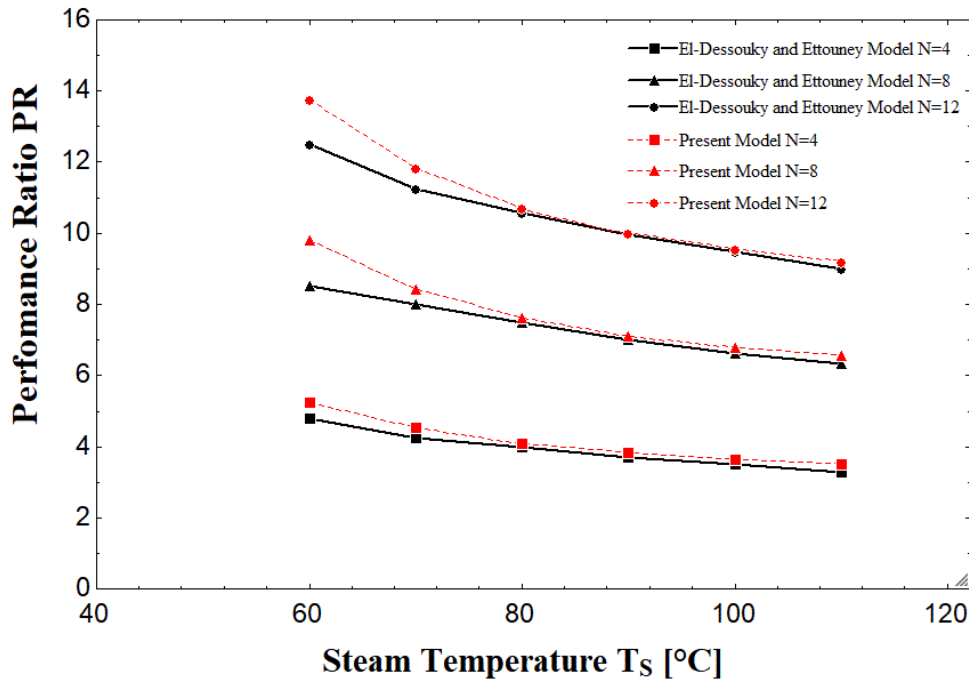


Figure 4. Effect of heating steam temperature and number of effects on the performance ratio of El-Dessouky and Ettouney (2002) and present model.

Performance ratio of the present model of MED and MED-TVC are compared for different steam temperatures and number of effects in Fig. 6. The TVC extract a portion of the formed vapor formed in the last effect and mix it with motive steam, reducing the amount of motive steam used and increasing the performance ratio. Therefore, results show an increase up to 47 % in the performance ratio of MED-TVC model against the stand-alone MED system, in agreement with the results published in the literature (El-Dessouky and Ettouney, 2002).

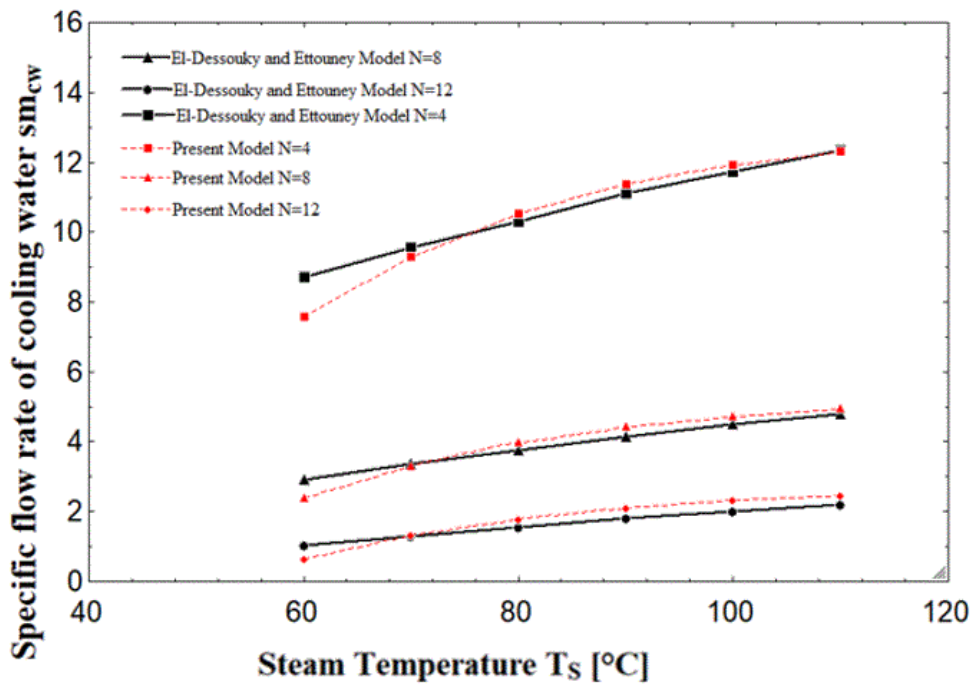


Figure 5. Effect of number of effects and steam temperature on the performance ratio of El-Dessouky and Ettouney (2002) and present model.

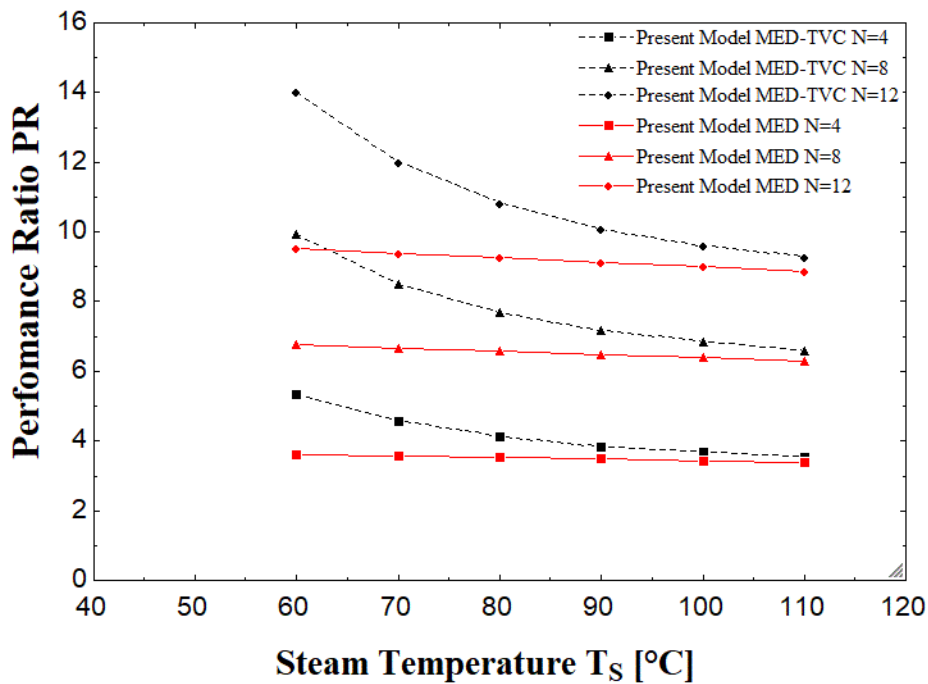


Figure. 6. Effect of heating steam temperature and the number of effects on the performance ratio of the MED and MED-TVC systems.

3.2 Rankine cycle parametric analysis

A parametric study based on E. P. Dall (2017) work is developed in order to reach the peak potential cycle efficiency. Configurations with different outlet steam temperatures (T_M) of the low-pressure turbine and inlet of MED system are evaluated in Tab. 3, the optimization procedure involves an iterative process in which the pressure values of the high-pressure turbine (HPT) and the feed heater bleeding locations are determined. The pressure optimization of each point is repeated until the value of Rankine efficiency reaches convergence, when the third significant figure stops varying. The results show that the highest efficiency is corresponding to the temperature $T_M = 60$ °C.

Table 3. Rankine cycle bleed-off optimization results

Point	$T_M = 60$ °C $\eta_{\text{rankine}} = 43.39$ %	$T_M = 65$ °C $\eta_{\text{rankine}} = 42.74$ %	$T_M = 70$ °C $\eta_{\text{rankine}} = 42.09$ %
HPT outlet (kPa)	6934	6934	6732
Closed FWH 1 (kPa)	5939	5980	6061
Closed FWH 2 (kPa)	3010	3035	3136
Direct contact FWH 3 (kPa)	1348	1379	1455
Closed FWH 4 (kPa)	375.8	393.9	436.4
Closed FWH 5 (kPa)	95.45	109.1	140.9

4. CONCLUSION

This paper presents a model to simulate part of a CSP plant working in cogeneration with a MED system, through a simultaneous equation solver. Parametric studies were developed and compared to the literature results in order to validate the models. Two different configurations of the MED model were considered, a standalone MED plant and a MED plant using a thermal vapor compressor.

The results showed that the MED models are in accordance with the expected behavior published in the literature by several authors, for parameters like the performance ratio and the specific flow rate of cooling water. Moreover, comparing the configurations with a standalone MED plant and a MED-TVC plant an increase up to 47 % in the performance ratio of MED-TVC is reported. The iterative procedure of the Rankine power generation cycle determined the optimized pressure bleed-off points in order to reach the highest cycle efficiency possible Tab. 3, and it was observed a significant variation in the pressure for each outlet steam temperature considered.

5. REFERENCES

- Blanco, J., Palenzuela, Alarcón-Padilla, D., Zaragoza, G., & Ibarra, M., 2013. *Preliminary thermoeconomic analysis of combined parabolic trough solar power and desalination plant in port Safaga (Egypt)*. *Desalination and Water Treatment*, 51(7-9), 1887–1899.
- Casimiro, S., Cardoso, J., Alarcón-Padilla, D. C., Turchi, C., Ioakimidis, C., & Mendes, J. F., 2014. *Modeling Multi Effect Distillation Powered by CSP in TRNSYS*. *Energy Procedia*, 49, 2241–2250.
- Darwish, M. A., Al-Juwayhel, F., & Abdulraheim, H. K., 2006. *Multi-effect boiling systems from an energy viewpoint*. *Desalination*, 194(1-3), 22-39.
- El-Dessouky, H. T., Ettouney, H. M., 2002. *Fundamentals of Salt Water Desalination*, Elsevier, Amsterdam, The Netherlands, 2002.
- El-Sayed, Y. M., Silver, R. S., 1980. *Principles of Desalination*. volume A, Academic Press, New York, NY, 2nd edition, pp. 55-109.
- Hoffmann, J. E., & Dall, E. P., 2017. *Integrating desalination with concentrating solar power: large scale cogeneration of water and electricity*. Stellenbosch University, Stellenbosch.
- Khalid, K. A., Antar, M. A., Khalifa, A., & Hamed, O. A., 2018. *Allocation of thermal vapor compressor in multi effect desalination systems with different feed configurations*. *Desalination*, 426, 164–173.
- Malagueta D., Szklo A., Soria R., Dutra R., Schaeffer R., Borba B. *Potential and impacts of Concentrated Solar Power (CSP) integration in the Brazilian electric power system*. *Renew Energy* 2014;68 (August 2014):223e35.
- Mistry, K. H., Antar, M. A., & Lienhard V, J. H., 2013. *An improved model for multiple effect distillation*. *Desalination and Water Treatment*, 51(4-6), 807–821.
- Olwig, R., Hirsch, T., Sattler, C., Glade, H., Schmeken, L., Will, S., Messalem, R., 2012. *Techno-economic analysis of combined concentrating solar power and desalination plant configurations in Israel and Jordan*. *Desalination and Water Treatment*, 41(1-3), 9–25.
- Power, R B., 1994. *Steam jet ejectors for the process industries*. United States.
- Sharqawy, M. H., Lienhard, J. H., & Zubair, S. M., 2010. *Thermophysical properties of seawater: a review of existing correlations and data*. *Desalination and Water Treatment*, 16(1-3), 354–380.
- Soria, R., Lucena, A.F.P., Tomaschek, J., Fichter, T., Haasz, T., Szklo, A., Schaeffer, R., Rochedo, P., Fahl, U., Kern, J., 2016. *Modelling concentrated solar power (CSP) in the Brazilian energy system: A soft-linked model coupling approach*. *Energy* 116, Part 1, 265– 280.
- Trieb, F., German Aerospace Center (DLR), 2007. *“Aqua-CSP Study Report, Concentrating Solar Power for Seawater Desalination, Final Report,”* German Aerospace Center (DLR), Stuttgart.
- U.S. Energy Information Administration (EIA), 2019. *International Energy Outlook 2019 with projections to 2050*. Office of Energy Analysis, U.S. Department of Energy, Washington, DC

6. RESPONSIBILITY NOTICE

The authors are the only responsible for the printed material included in this paper.